

HYDROGASDYNAMICS IN TECHNOLOGICAL PROCESSES

MODELING OF SWIRLING TURBULENT FLOW IN A SEPARATOR WITH BICONICAL PLATES

A. V. Shvab and A. G. Chepel^{*}

UDC 532.517.4

Turbulent swirling flow in the gap between rotating cones, which represents the working element of a plate-type centrifugal separator, is modeled numerically. On the basis of the introduced orthogonal biconical coordinate system, numerical solution of the Reynolds equations is modeled; these equations are closed using the well-known Wilcox differential two-parameter $k-\omega$ turbulence model. The results of the numerical solution are represented in the form of the distribution of the averaged velocity components and the characteristic turbulence parameters as functions of the operating and geometric parameters in the separator's working element; the reliability of the results is confirmed by comparing to test calculations and to the existing experimental data.

Keywords: turbulent flow, biconical coordinate system, spaced grid, separator, centrifugal force, turbulent stresses, generalized alternating-direction method.

Introduction. Swirling turbulent flows in vortex chambers, separators, and air-centrifugal classifiers are of practical interest when powders of certain granulometric composition are produced. Active development of the promising industrial trends and of new materials with prescribed properties has much to do with the progress made in the field of production of finely dispersed powders of certain size. Improvement and technological evolution of the processes of separation and classification of finely dispersed powder materials are impossible without a thorough theoretical investigation of the hydrodynamics of the carrier medium. In actual practice, flows in apparatuses using flow swirl are turbulent in most cases. Therefore, it is important to select a turbulence model. An analysis of numerical and experimental investigations shows that the hydrodynamics of a swirling flow exerts a decisive influence on the separation. Therefore, creation of real aerodynamic conditions in the working chamber of a centrifugal apparatus is an important aspect of numerical modeling of such a flow. Only a joint experimental and theoretical investigation of swirling turbulent flows can enable one to understand the essence of the processes in them and to reveal new approaches to their theoretical description. The present work seeks to investigate in detail the velocity field of swirling turbulent flow in the working chamber of a biconical separator.

Physical and Mathematical Formulation of the Problem. We model swirling turbulent flow in the gap between two rotating cones, which is the working element of a plate-type centrifugal separator. The propagation of the flow in the region in question is shown in Fig. 1. Under the action of the pressure difference, the gas enters, from the periphery (boundary B_1), the interplate gap formed by two cones (boundaries B_2 and B_3) and escapes through boundary B_4 . The exterior and interior cone walls rotate with a prescribed angular velocity Ω_d . We will assume that the angular rotational velocity of the gas Ω_g at the inlet boundary B_1 is known. The angle α represents the half-angle of opening of coaxially arranged rotating cones. In the limiting case for $\alpha = \pi/2$ the region in question becomes the gap between plane rotating disks. This case is also considered in the present work. We emphasize that the flow under study is symmetric in the circumferential direction; therefore, we have $\partial/\partial\varphi = 0$.

Swirling turbulent flow in the region in question is conveniently described in the orthogonal biconical coordinate system η, φ, χ first introduced apparently by Gol'din [1]. The Cartesian coordinates x, y, z are linked to the biconical ones by the following relations:

Tomsk State University, 36 Lenin Ave., Tomsk, 634050, Russia; email: anton232@yandex.ru. Translated from Inzhenerno-Fizicheskii Zhurnal, Vol. 83, No. 2, pp. 318–325, March–April, 2010. Original article submitted July 13, 2009.

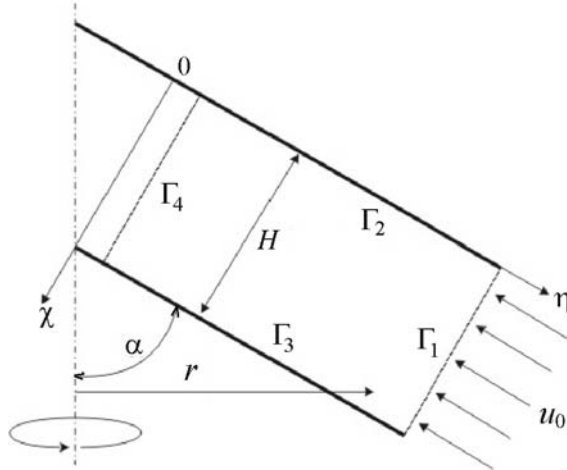


Fig. 1. Diagram of the working area of a biconical separator.

$$x = (\eta \sin \alpha - \chi \cos \alpha) \cos \varphi, \quad y = (\eta \sin \alpha - \chi \cos \alpha) \sin \varphi, \quad z = \eta \cos \alpha - \chi \sin \alpha. \quad (1)$$

Computing the Lame' coefficients for the orthogonal biconical coordinate system, we obtain

$$H_\chi = H_\eta = 1, \quad H_\varphi = \eta \sin \alpha - \chi \cos \alpha,$$

the distance from the axis to an arbitrary point in the region in question is coincident with the Lame' coefficient H_φ , i.e., we have

$$r = H_\varphi = \eta \cos \alpha - \chi \sin \alpha.$$

Using the analytical representations of space derivatives in orthogonal curvilinear coordinates (1) and representing the actual values of velocities and pressure by the sum of the time-averaged and pulsation components, after the procedure of Reynolds averaging of the equations, we obtain the averaged Navier-Stokes equations in the biconical coordinate system for axisymmetric flow in the following form:

the continuity equation

$$\frac{\partial}{\partial \eta} (r u_\eta) + \frac{\partial}{\partial \chi} (r u_\chi) = 0, \quad (2)$$

and the momentum-transfer equations with allowance for axial symmetry ($\partial/\partial\varphi = 0$)

$$\begin{aligned} \frac{\partial u_\eta}{\partial t} + u_\eta \frac{\partial r u_\eta}{\partial \chi} - \frac{u_\varphi^2}{r} \sin \alpha &= -\frac{1}{\rho} \frac{\partial p}{\partial \eta} + \frac{\cos \alpha}{r} \overline{u'_\eta u'_\chi} \\ -\frac{\sin \alpha}{r} \left(\overline{u_\eta'^2} - \overline{u_\varphi'^2} \right) - \frac{\partial \overline{u'_\eta u'_\chi}}{\partial \chi} + v \left[\nabla^2 u_\eta + \frac{\sin \alpha}{r} \left(\frac{u_\chi}{r} \cos \alpha - \frac{u_\eta}{r} \sin \alpha \right) \right], \end{aligned} \quad (3)$$

$$\begin{aligned} \frac{\partial u_\varphi}{\partial t} + u_\eta \frac{\partial u_\varphi}{\partial \eta} + u_\chi \frac{\partial u_\varphi}{\partial \chi} + \frac{u_\eta u_\varphi}{r} \sin \alpha - \frac{u_\chi u_\varphi}{r} \cos \alpha &= -\frac{\partial \overline{u'_\eta u'_\varphi}}{\partial \eta} - \frac{\partial \overline{u'_\chi u'_\varphi}}{\partial \chi} \\ -\frac{2}{r} \sin \alpha \overline{u'_\eta u'_\varphi} + \frac{2}{r} \cos \alpha \overline{u'_\chi u'_\varphi} + v \left(\nabla^2 u_\varphi - \frac{1}{r} \frac{u_\varphi}{r} \right), \end{aligned} \quad (4)$$

$$\begin{aligned}
& \frac{\partial u_\chi}{\partial t} + u_\eta \frac{\partial u_\chi}{\partial \eta} + u_\chi \frac{\partial u_\chi}{\partial \chi} + \frac{u_\varphi^2}{r} \cos \alpha = -\frac{1}{\rho} \frac{\partial p}{\partial \chi} + \frac{\cos \alpha}{r} \left(\overline{u_\chi'^2} - \overline{u_\varphi'^2} \right) \\
& - \frac{\partial \overline{u_\eta' u_\chi'}}{\partial \eta} - \frac{\partial \overline{u_\chi'^2}}{\partial \chi} - \frac{\sin \alpha}{r} \overline{u_\chi' u_\eta'} + v \left[\nabla_t^2 u_\chi + \frac{\cos \alpha}{r} \left(\frac{u_\eta}{r} \sin \alpha - \frac{u_\chi}{r} \right) \right], \\
\nabla^2 & \equiv \frac{1}{r} \frac{\partial}{\partial \eta} \left(r \frac{\partial}{\partial \eta} \right) + \frac{1}{r} \frac{\partial}{\partial \chi} \left(r \frac{\partial}{\partial \chi} \right).
\end{aligned} \tag{5}$$

The obtained system of equations (2)–(5) is open; therefore, we must use supplementary hypotheses for linking the resulting components of the Reynold-stress tensors to the characteristics of the averaged flow. The generalized Boussinesq hypothesis is known to be highly efficient for practical engineering calculations; according to this hypothesis, Reynolds stresses are assumed to be proportional to the strain rate of the averaged flow with an unknown proportionality factor μ which is called the coefficient of turbulent, "apparent" viscosity:

$$\tau_{ij} = -\rho \overline{u_i' u_j'} = \mu_t \left(\frac{\partial u_i}{\partial x_j} + \frac{\partial u_j}{\partial x_i} \right) - \frac{2}{3} \rho \delta_{ij} k. \tag{6}$$

Replacing the turbulent stresses in system (2)–(5) using the generalized Boussinesq hypothesis (6), we obtain a system of Reynolds equations that will be represented in conservative divergent form:

$$\frac{\partial}{\partial \eta} (r u_\eta) + \frac{\partial}{\partial \chi} (r u_\chi) = 0, \tag{7}$$

$$\begin{aligned}
& r \frac{\partial u_\eta}{\partial t} + \frac{\partial r u_\eta^2}{\partial \eta} + \frac{\partial r u_\eta u_\chi}{\partial \chi} - \nabla_t^2 u_\eta = -r \frac{\partial p}{\partial \eta} + u_\varphi^2 \sin \alpha + r \frac{\partial v_t}{\partial \eta} \frac{\partial u_\eta}{\partial \eta} \\
& + r \frac{\partial v_t}{\partial \chi} \frac{\partial u_\chi}{\partial \eta} + \frac{(v + v_t)}{r} (u_\chi \cos \alpha \sin \alpha - u_\eta \sin^2 \alpha) - r \frac{2}{3} \frac{\partial k}{\partial \eta},
\end{aligned} \tag{8}$$

$$\begin{aligned}
& r \frac{\partial u_\varphi}{\partial t} + \frac{\partial r u_\eta u_\varphi}{\partial \eta} + \frac{\partial r u_\chi u_\varphi}{\partial \chi} - \nabla_t^2 u_\varphi = -u_\eta u_\varphi \sin \alpha + u_\chi u_\varphi \cos \alpha - \frac{\partial v_t}{\partial \eta} u_\varphi \sin \alpha \\
& + \frac{\partial v_t}{\partial \chi} u_\varphi \cos \alpha - (v + v_t) \frac{u_\varphi}{r},
\end{aligned} \tag{9}$$

$$\begin{aligned}
& r \frac{\partial u_\eta}{\partial t} + \frac{\partial r u_\eta u_\chi}{\partial \eta} + \frac{\partial r u_\chi^2}{\partial \chi} - \nabla_t^2 u_\chi = -r \frac{\partial p}{\partial \chi} - u_\varphi^2 \cos \alpha + r \frac{\partial v_t}{\partial \eta} \frac{\partial u_\eta}{\partial \chi} \\
& + r \frac{\partial v_t}{\partial \chi} \frac{\partial u_\chi}{\partial \eta} + \frac{(v + v_t)}{r} (u_\eta \cos \alpha \sin \alpha - u_\chi \cos^2 \alpha) - r \frac{2}{3} \frac{\partial k}{\partial \chi},
\end{aligned} \tag{10}$$

$$\nabla_t^2 = \frac{\partial}{\partial \eta} \left[r (v + v_t) \frac{\partial}{\partial \eta} \right] + \frac{\partial}{\partial \chi} \left[r (v + v_t) \frac{\partial}{\partial \chi} \right]. \tag{11}$$

To determine the turbulent, "apparent" viscosity we will use a rather popular and verified Wilcox turbulence model [2] that contains the transfer equations for the kinetic energy of pulsatory motion of the flow k and the specific rate of kinetic-energy dissipation ω . In the biconical coordinate system, this turbulence model will have the form

$$\begin{aligned} r \frac{\partial k}{\partial t} + \frac{\partial r u_\eta k}{\partial \eta} + \frac{\partial r u_\chi k}{\partial \chi} - \frac{\partial}{\partial \eta} \left[r \left(v + \frac{v_t}{\sigma^*} \right) \frac{\partial k}{\partial \eta} \right] - \frac{\partial}{\partial \chi} \left[r \left(v + \frac{v_t}{\sigma^*} \right) \frac{\partial k}{\partial \chi} \right] \\ = G - \frac{2}{r} \left(\frac{2}{3} k + v_t \frac{\partial u_\chi}{\partial \chi} \right) - r \beta^* k \omega, \end{aligned} \quad (12)$$

$$r \frac{\partial \omega}{\partial t} + \frac{\partial r u_\eta \omega}{\partial \eta} + \frac{\partial r u_\chi \omega}{\partial \chi} - \frac{\partial}{\partial \eta} \left[r \left(v + \frac{v_t}{\sigma} \right) \frac{\partial \omega}{\partial \eta} \right] - \frac{\partial}{\partial \chi} \left[r \left(v + \frac{v_t}{\sigma} \right) \frac{\partial \omega}{\partial \chi} \right] = \frac{\omega}{k} G \gamma - r \beta \omega^2, \quad (13)$$

$$\begin{aligned} v_t = \frac{k}{\omega}; \quad G = r v_t \left\{ 2 \left[\left(\frac{\partial u_\eta}{\partial \eta} \right)^2 + \left(\frac{\partial u_\chi}{\partial \chi} \right)^2 + \left(\frac{u_\eta}{r} \sin \alpha - \frac{u_\chi}{r} \cos \alpha \right)^2 \right] \right. \\ \left. + \left(\frac{\partial u_\phi}{\partial \eta} - \frac{u_\phi}{r} \sin \alpha \right)^2 + \left(\frac{\partial u_\phi}{\partial \chi} + \frac{u_\phi}{r} \cos \alpha \right)^2 + \left(\frac{\partial u_\chi}{\partial \eta} + \frac{\partial u_\eta}{\partial \chi} \right)^2 \right\}. \end{aligned}$$

Here the constants of the turbulence model have the values $\beta = 3/40$, $\beta^* = 0.09$, $\sigma = 2$, $\sigma^* = 2$, and $\gamma = 5/9$ [2].

Thus, Eqs. (7)–(11) and (12), (13) represent a closed system of differential equations describing axisymmetric swirling turbulent flow of an incompressible fluid in the biconical coordinate system.

Selecting the value of the meridional velocity $(u_\eta)_{av} = u_0$ at the inlet boundary B_1 as the velocity scale and the distance between the cones H as the length scale, we obtain the dimensionless form of Eqs. (7)–(11) and (12), (13) which contain one criterion: the Reynolds number of the form $Re = u_0 H / v$.

To obtain a unique solution at the boundaries of the region under study we use the following boundary conditions. A constant value of the velocity $u_\eta = -u_0$ (or, in dimensionless form, $u_\eta^* = -1$) is prescribed at the inlet boundary (B_1) for the meridional velocity; here and in what follows * denotes dimensionless quantities. The condition $\partial u_\chi / \partial \eta = 0$ is used for the transverse velocity component, and $u_\phi = \Omega_g r_0$ (or, in dimensionless form, $u_\phi^* = R_g r_0^*$, where $r_0^* = r_0 / H$ and $R_g = \Omega_g H / u_0$ is the inverse Rossby number) is used for the circumferential velocity component. We prescribe constant values for the dimensionless values of kinetic energy $k_0^* = k_0 / u_0^2$ and its specific dissipation rate $\omega_0^* = \omega_0 H / u_0$ at the inlet boundary. A "soft" condition $(\partial / \partial \eta = 0)$ is used for all variables at the outlet boundary (B_4). On the walls (B_2 and B_3), we use the adhesion condition for the variables u_η^* , u_χ^* , and k^* , i.e., $u_\eta^* = u_\chi^* = k^* = 0$. For the circumferential velocity component, we use the expression $u_\phi^* = R_d r_w^*$, where $R_d = \Omega_d H / u_0$ is the inverse Rossby criterion characterizing the swirl of the walls and $r_w^* = r_w / H$, r_w is the wall's running radius. The specific dissipation rate ω on a solid surface is determined from the initial transfer equation. In this case the boundary condition for the specific dissipation rate on a solid wall is reduced to the balance between molecular diffusion and dissipation:

$$\frac{\partial}{\partial \chi} \left(r \frac{\partial \omega}{\partial \chi} \right) = r \operatorname{Re} \beta \omega^2.$$

Thus, the numerical solution of the problem is dependent on the criteria Re , R_g , R_d , k_0^* , and ω_0^* .

Method of Solution. The numerical solution of the system of differential equations (7)–(11) and (12), (13) is carried out in "velocity–pressure" physical variables by physical splitting of the velocity and pressure fields [3]. According to this method, the solution of the Reynolds equations written in vector form is subdivided into two steps:

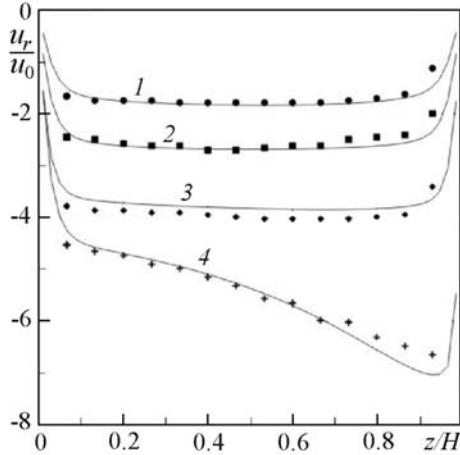


Fig. 2. Comparison of the calculated radial velocity component to experimental data for the flow rate $Q = 0.01971 \text{ m}^3/\text{sec}$ in four cross sections: 1) $r/r_0 = 0.6$, 2) 0.4, 3) 0.275, and 4) 0.185.

$$\frac{\mathbf{V}^+ - \mathbf{V}^n}{\Delta t} + = -\nabla p^n + F(\mathbf{V}^+, \mathbf{V}^n), \quad (14)$$

$$\frac{\mathbf{V}^{n+1} - \mathbf{V}^+}{\Delta t} = -\nabla(\Delta p). \quad (15)$$

Equation (14) represents the system of equations (8)–(10) in symbolic form and vector form. Here $^+$ denotes the intermediate grid function for the velocity vector and $\Delta p = p^{u+1} - p^n$ is the pressure correction. Multiplying (15) by the gradient and taking account of the solenoidal character of the velocity vector on the $(n+1)$ th time layer, we obtain the Poisson equation for determination of the pressure correction

$$\nabla^2(\Delta p) = \frac{\nabla \cdot \mathbf{V}^+}{\Delta t}. \quad (16)$$

The solution of the steady-state problem is carried out by the method of establishment with time; therefore, dependence (16) is written in the form of the nonsteady differential equation

$$\frac{\partial \Delta p}{\partial \tau} - \nabla^2(\Delta p) = -\frac{\nabla \cdot \mathbf{V}^+}{\Delta t}, \quad (17)$$

in which τ is the fictitious time acting as the iteration parameter. When Eq. (7) is solved the time step can be determined as $\Delta\tau = A\Delta t$; in this case the value of the constant A is less than unity as a rule and is selected from the condition of a faster convergence process. For the pressure correction we use, as the boundary condition, the Neumann condition, which is satisfied if the exact value of \mathbf{V}^{n+1} is used for \mathbf{V}^+ at the boundary, as has been shown in [4].

Thus, in the first step, we have solved, by the establishment method, the system of equations (14) and then Eqs. (17) and (15) have determined the velocity vector on the $(n+1)$ th time layer and the pressure $p^{n+1} = p^n + \Delta p$.

The method of splitting of the velocity and pressure fields yields the system of equations (8)–(13) and (17), with each equation of this system representing the equation of transfer of a scalar substance. The transfer equation is written in conservative divergent form. Numerical solution is carried out on a hybrid staggered difference grid by the control-volume method. The convective and diffusive terms of this equation are represented in finite differences using the exponential scheme [5]. This scheme ensures the second order of accuracy in coordinates and lifts the restriction on the grid Reynolds number.

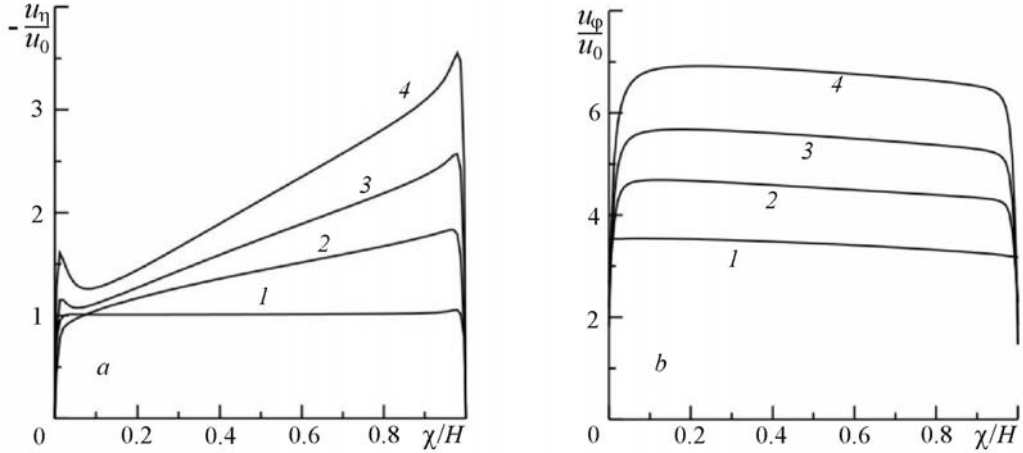


Fig. 3. Evolution of the meridional (a) and circumferential (b) velocities with coordinate χ for the parameters $Re = 5000$, $R_d = 0.5$, and $R_g = 0.5$ in four cross sections: 1) $\eta/\eta_0 = 0.99$, 2) 0.75, 3) 0.625, and 4) 0.5.

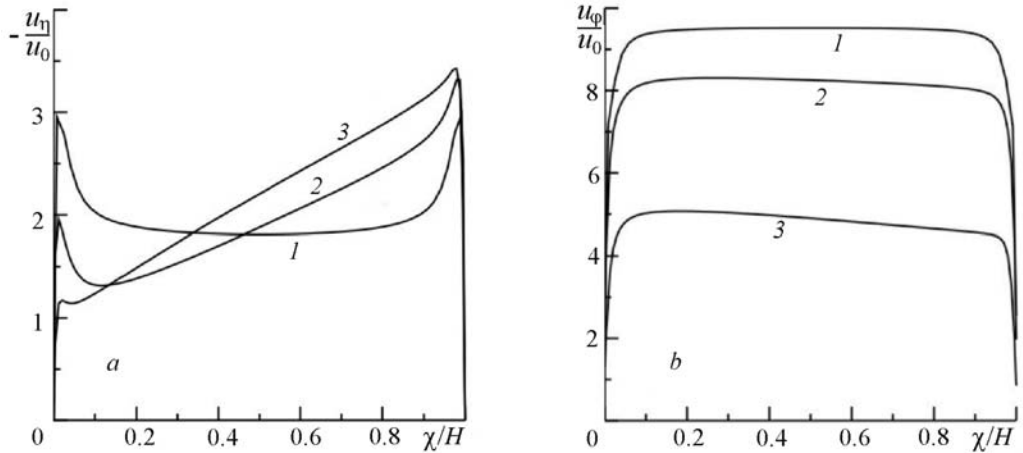


Fig. 4. Influence of the slope α on the meridional (a) and circumferential (b) velocities vs. coordinate χ in the outlet cross section for the parameters $Re = 5000$, $R_d = 0.5$, and $R_g = 0.5$: 1) $\alpha = \pi/2$, 2) $\pi/3$, and 3) $\pi/6$.

Numerical Results. In the work, we present test investigations of the obtained results for reliability. Thus, Fig. 2 compares experimental data [6] and calculation for the limiting case of turbulent flow directed from the periphery toward the axis of symmetry between parallel disks ($\alpha = \pi/2$). For this case, the biconical orthogonal coordinate system (1) automatically becomes a cylindrical one ($\eta = r$, $\chi = z$).

Figure 3 shows the evolution of the averaged meridional and circumferential velocities with coordinate χ for different η/η_0 values. It is clear from the plot that the flow core and two asymmetric boundary layers near the solid surfaces of the rotating cones are formed in the biconical element in the case of flow. This difference in the circumferential-velocity profile produces the inhomogeneity of the field of centrifugal forces and as a consequence initiates the velocity maxima of the meridional component in the boundary layers where the level of centrifugal force is lower. The value of linear circumferential velocity on the wall of the internal cone is much smaller than that on the exterior wall due to the difference in the distance to the axis of rotation. Therefore, the maximum of meridional velocity near the internal cone is much larger due to the lower level of centrifugal force.

The influence of the angle of opening of the biconical element α on the evolution of the meridional and circumferential velocity components is shown in Fig. 4; it is seen that the maximum level of circumferential velocities is attained for the angle $\alpha = \pi/2$, which corresponds to flow between plane-parallel disks. As the slope of the biconical element α decreases, the symmetric distribution of the meridional velocity is broken and its inhomogeneity increases.

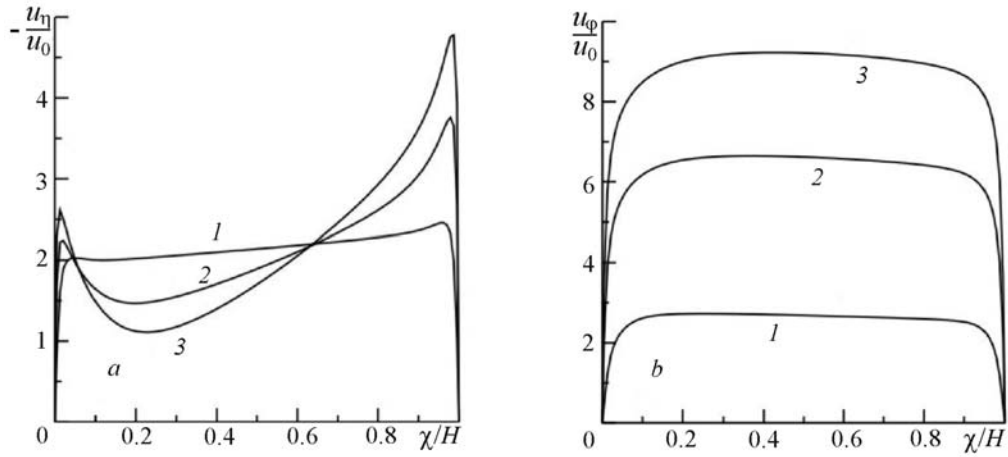


Fig. 5. Influence of the swirl parameter of the gas R_g on the meridional (a) and circumferential (b) velocities vs. coordinate χ in the outlet cross section for the parameters $Re = 5000$, $R_d = 0$, and $\alpha = \pi/4$: 1) $R_g = 0.2$, 2) 0.5 , and 3) 0.7 .

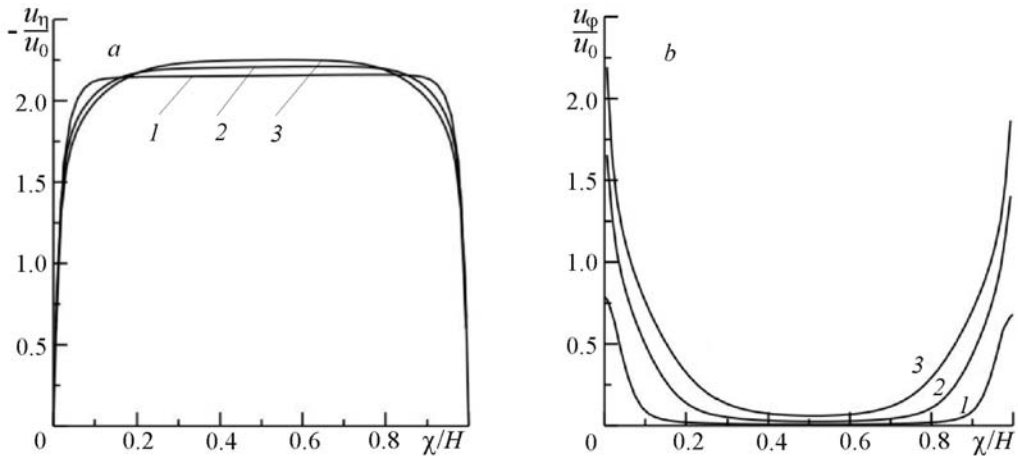


Fig. 6. Influence of the swirl parameter of the disks R_d on the meridional (a) and circumferential (b) velocities vs. coordinate χ in the outlet cross section for the parameters $Re = 5000$, $R_g = 0.5$, and $\alpha = \pi/4$: 1) $R_d = 0.2$, 2) 0.5 , and 3) 0.7 .

The influence of the rotation parameters R_d and R_g on the averaged-velocity field is shown in Fig. 5 and Fig. 6. More intense rotation of the cones (increase in R_d) causes the level of circumferential velocities in the boundary layers to increase, which somewhat smooth the profile of meridional velocity in these regions. Increase in the inlet circumferential gas velocity characterized by the dimensionless rotation parameter R_g leads to a more intense growth in the centrifugal forces in the flow core, with the result that the inhomogeneity of the meridional-velocity profile increases.

Conclusions. The developed mathematical model of steady-state swirling turbulent flow in the gap between rotating cones can be used in optimizing operating and geometric parameters in separators with biconical plates and in air-centrifugal classifiers and when new structures of powder-technology apparatuses are developed.

NOTATION

H , height scale of the separator's working area, m; H_η , H_χ , and H_ϕ , Lame' coefficients; k , kinetic energy of pulsatory motion, m^2/sec^2 ; k^* , dimensionless kinetic energy of pulsatory motion; k_0 , constant, kinetic turbulent-pulsation energy prescribed at entry, m^2/sec^2 ; p , pressure, Pa; Q , volumetric flow rate of the gas, m^3/sec ; r , radius, dis-

tance from the axis of rotation to the arbitrary point, m; Re , Reynolds criterion; R_d and R_g , Rossby numbers expressing the dimensionless angular rotational velocity of disk elements and the dimensionless average angular velocity of the gas at entry into the apparatus chamber respectively; t , time coordinate, sec; u_η , u_χ , and u_ϕ , velocity-vector components in biconical coordinates, m/sec; u_η^* , u_χ^* , and u_ϕ^* , dimensionless velocity-vector components; u_r , u_z , and u_ϕ , velocity-vector components in cylindrical coordinates, m/sec; u_0 , mean-flow-rate value of the inlet velocity, m/sec; \mathbf{V} , velocity vector; \mathbf{V}^+ , intermediate value of the velocity vector; x , y , z , Cartesian coordinates; α , slope of biconical plates with respect to the axis of rotation; $\beta = 3/40$; $\beta^* = 9/100$; $\gamma = 5/9$; δ_{ij} , Kronecker symbol; η , χ , ϕ , biconical coordinates; ν , coefficient of kinematic viscosity, m²/sec; ν_t , coefficient of turbulent viscosity, m²/sec; ρ , gas density, kg/m³; $\sigma = 2$; $\sigma^* = 2$; Ω_d , angular velocity of disk elements, 1/sec; Ω_g , average angular velocity of the gas at entry into the apparatus, 1/sec; ω , angular rate of dissipation of the kinetic energy of pulsatory motion, 1/sec; ∇^2 and ∇_t^2 , Laplacians. Subscripts: i and j , numbers of grid nodes along the coordinates η and χ ; n , previous time layer in the difference scheme; $n + 1$, new time layer in the difference scheme; w , wall; g , gas; d , disk; t , turbulent; 0 , inlet parameters; av , average, mean.

REFERENCES

1. E. M. Gol'din, Stability of the flow between separator plates, *Izv. Akad. Nauk SSSR, Mekh. Zhidk. Gaza*, No. 2, 152–155 (1966).
2. D. C. Wilcox, Reassessment of the scale-determining equation for advanced turbulence models, *AIAA J.*, **26**, No. 11, 1299–1310 (1988).
3. A. J. Chorin, Numerical solution of Navier–Stokes equation, *Math. Comput.*, **22**, 745–762 (1968).
4. R. Peyret and T. D. Taylor, *Computational Methods for Fluid Flow* [Russian translation], Gidrometeoizdat, Leningrad (1986).
5. S. Patankar, *Numerical Methods for Solving Problems of Heat Transfer and Fluid Dynamics* [Russian translation], Énergoatomizdat, Moscow (1984).
6. A. Singh, B. D. Vyas, and U. S. Powle, Investigations on inward flow between two stationary parallel disks, *Int. J. Heat Fluid Flow*, No. 20, 395–401 (1999).